VARIATION OF AEROSOL OPTICAL AND MICROPHYSICAL PROPERTIES IN KISHINEV DURING THE SAHARAN DUST OUTBREAK INTO EUROPE ON OCTOBER 30, 2001

Aculinin A.

Atmospheric Research Group (ARG), Institute of Applied Physics, Academy of Sciences of Moldova, 5 Academiei Str., Kishinev MD-2028 Moldova, e-mail: akulinin@phys.asm.md

Abstract

Atmospheric aerosol optical and microphysical properties derived from the direct Sun and diffuse sky radiance measurements at the Kishinev site are investigated. These properties are analyzed in connection with the Saharan dust outbreak into Europe occurred on October 30, 2001. The work was done within the frame of the Aerosol Robotic Network (AERONET) program from the NASA/Goddard Space Flight Center (GSFC).

1. Introduction

Atmospheric aerosols both from anthropogenic (e.g., black carbon, sulfate, biomass burning smokes, fossil fuel combustion, soil dust) and natural (e.g., sea salt, mineral dust, volcanoes ash) sources possess large temporal and regional variability in their optical and microphysical properties. Variability of atmospheric aerosols properties results from the complex interaction of the synoptic processes, which are responsible for the air masses transport and transformation, with the processes that initially form these aerosols both with anthropogenic and natural origin. Aerosols play essential role in the heat balance of the Earth by (a) scattering and absorbing of incoming solar radiation, and (b) by representing as condensation nuclei for clouds formation [1]. Global radiative forcing due to aerosols is evaluated as ~ -1.6 ± 1.3 Wm^{-2}, which approximately compensates the mean global radiative forcing due to greenhouse gas warming amounting to ~2.4 ± 0.3 Wm^{-2} [2].

Each of aerosol components makes specific contribution to the radiative forcing. Estimates of dust contribution into the overall particle emissions vary from 1000 to 5000 Mt/year with high spatial and temporal variability. Value of the global radiative forcing due to dust aerosols varies from -0.6 Wm^{-2} to $+ 0.4$ Wm^{-2} . In general, the evaluation for dust aerosol is complicated by the fact that the short-wave contribution consists of a significant reflection and absorption component, and the long-wave exerts a substantial contribution by way of a trapping of the infrared radiation [2]. The large uncertainties with the respect to radiative forcing are stipulated with the dust production mechanisms, the properties of dust particles, and their evolution during the long-path transport [3]. Dust source regions are mainly deserts, dry lake beds, and semi-arid desert fringes. Major dust sources are found in the desert regions of the northern hemisphere, where the Sahara desert region represents as one of the most extensive sources of mineral dust [4]. Regular observations by the European Aerosol Research Lidar Network (EARLINET) showed rather frequent events of the Saharan desert dust transport from the southern to the northern Europe [5].

In this paper it is investigated variation of the aerosol optical and microphysical properties for the cloudless atmosphere derived from the direct Sun and diffuse sky radiance measurements. Specific column-integrated aerosol optical properties over the Kishinev site, Moldova, during the Saharan dust outbreak and its intrusion into Europe are analyzed.

2. Method

Column-integrated aerosol optical and microphysical properties, such as spectral aerosol optical thickness (AOT) $\tau_a(\lambda)$, Ångström exponent α(440_870), single scattering albedo ω_λ, asymmetry factor, complex refractive index *m=n-ik* and volume size distribution dV/dlnR, have been derived from the direct Sun and diffuse sky radiance almucantar measurements. These measurements have been carrying out at the Kishinev site, Moldova (47.00^{o}N, 28.82^{o}E; 205 m a.s.l.) since September 1999. This site is in operation in framework of the AERONET - globally distributed ground based network of radiometers to fulfill continuous monitoring of the aerosol optical properties [6]. AERONET team from the NASA/GSFC provided Kishinev site with the automatic Sun/sky scanning sunphotometer CIMEL CE-318 (Figure 1).

Figure 1. Sunphotometer CIMEL CE-318 in operation at the Kishinev site (47.00^{o}N, 28.82^{o}E; 205 m a.s.l.).

Sunphotometer makes direct Sun measurements in eight spectral channels at λ= 340, 380, 440, 500, 670, 870, 940 and 1020 nm. AOT $\tau_a(\lambda)$ is retrieved by using method being widely applied in Sun photometry[6]. Channel at 940 nm is used to retrieve precipitable water vapour content. Uncertainty in AOT $\tau_a(\lambda)$ measurements consists of value $\delta\tau_a(\lambda)$= 0.01-0.02 and has spectral dependence with high errors in the UV spectral range. In addition to the direct spectral measurements, sunphotometer makes diffuse sky radiance measurements in the solar almucantar and principal plane in four spectral channels within the spectral range from 440 to 1020 nm. The bandwidths of the solar radiometer's interference filters are varied from 2 nm (UV channels) to 10 nm (for visible and near-IR channels) at FWHM [6,7].

Kishinev site of observation is placed in the region where the Saharan dust outbreak trajectory has crossed it due to the complex movement and interaction of air masses. This dust outbreak initially originated in the Saharan desert region has intruded into Europe (Figure 2). As a rule Saharan dust intrusions are rather regular phenomena and have intense influence upon the aerosol optical properties [8-11]. At the same time, Saharan dust event in the late of October 2001 had discernable effect on column-integrated aerosol optical and microphysical properties over Moldova because of air mass transport of dust from Europe. In order to imagine how the dust was long-distance transported from the Saharan region to the Moldova, the 5-days backward trajectories of air masses were computed using the Hybrid Single Particle Lagrangian Integrated Trajectory (HYSPLIT) model (http://www.arl.noaa.gov/ready/hysplit4.html). Ending date for this backward trajectory modeling was chosen as October 31, 2001 (1200 UTC) and final results are shown in Figure 3. From this figure it is clearly seen how air masses with the Saharan desert dust have been transported to Moldova. The end point of these trajectories is located in Kishinev and is marked by star.

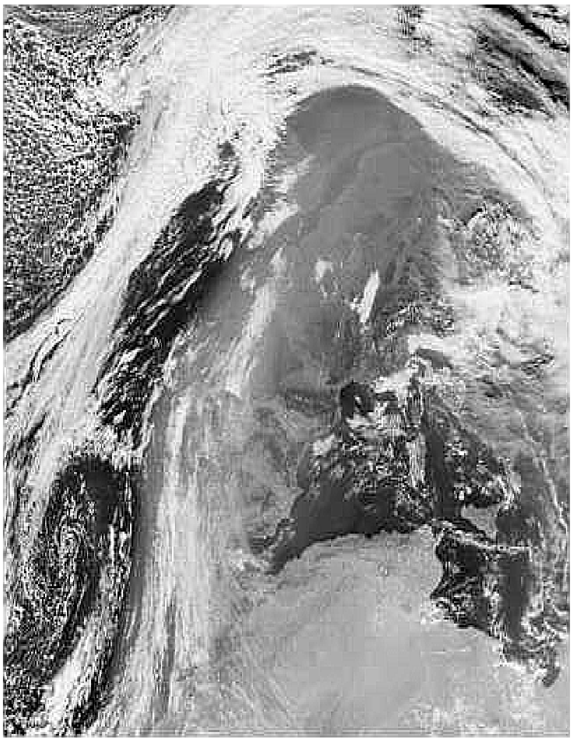

Figure 2. Composite satellite image of the Saharan dust outbreak into the Europe on 30/10/2001 (from SeaWiFS Project, NASA/GSFC, http://www.nrlmry.navy.mil/aerosol/Case_Studies/20011030_eur).

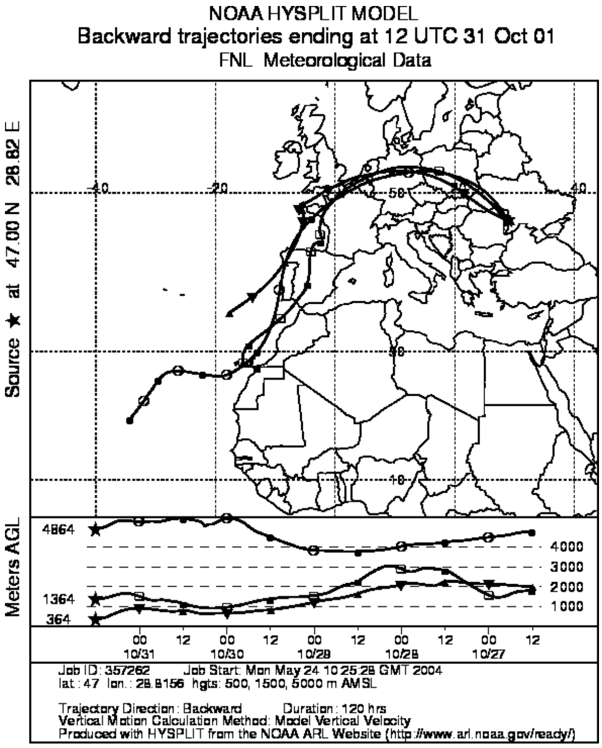

Figure 3. The 5-days back trajectories of air masses from the NOAA HYSPLIT modeling.

Period of observation from October 26, 2001 to November 5, 2001 was chosen as a week before and after the day of the Saharan dust outbreak in order to reveal the effect of the dust particulates. Data sets collected from the direct Sun and diffuse sky radiance almucantar measurements were used to determine variation of the column-integrated aerosol optical properties, such as of AOT $\tau_a(\lambda)$, Angstrom exponent $\alpha(440\_870)$, single scattering albedo ω_λ and complex refractive index, $m=n-ik$. Radiance measurements were carried out with the sunphotometer at the Kishinev site. These measurements were processed on cloud screening and quality control [12]. Column-integrated aerosol optical and microphysical properties were computed using the AERONET smart inversion algorithms [13,14] for the model of spheroidal particles because of numerous studies indicate the necessity to take into account for the particle non-sphericity in modeling of the optical properties of dust-like aerosols [9,15-17].

3. Results of measurements

Column-integrated volume size distributions dV/dlnR, for three days of observations on October 26 and 31, and November 5, 2001, were retrieved from the combined direct Sun and sky radiance almucantar measurements by using inversion procedures [13,14]. Results of retrieving are shown in Figure 4. Volume size distributions of desert dust always feature the bimodal structure with predominance of large particles of the coarse mode sizes [9]. It is likely, that one of the reasons of such bimodal structure consists in the mixture of desert dust with the anthropogenic pollutions in the boundary layer of the atmosphere. These pollutions can be of local origin or accumulated along the path of transport. Accordingly, in contrast to the urban and biomass burning aerosols, retrieved optical properties have specific features, e.g. Ångström exponent is low and ranges from 1.2 to -0.1, and phase function has high asymmetry factor at all wavelengths [9]. Main parameters of the retrieved columnar microphysical characteristics of aerosol particles at the Kishinev site for three selected days of observations are presented in Table 1.

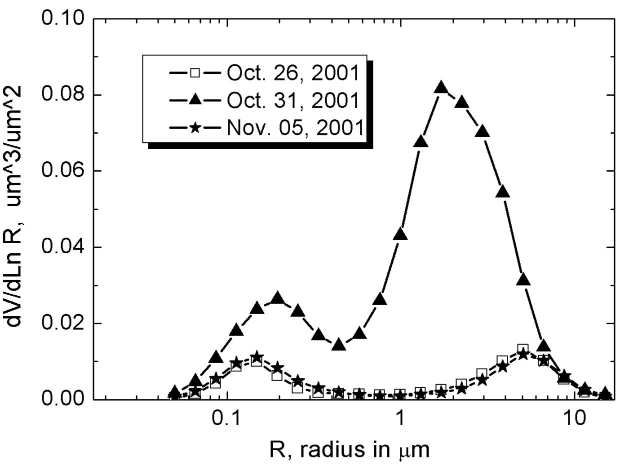

Figure 4. Daily average columnar volume size distributions, dV/dlnR retrieved from direct Sun and sky radiance almucantar measurements at the Kishinev site for three days of observations.

These parameters are retrieved separately for fine and coarse modes, and for total distribution. Parameters are selected as standard ones [7,9]: C_V is the volume concentration, $\mu m^3/\mu m^2$; R_V is the volume median radius (or mean logarithm of radius), μm; R_{eff} is the effective radius, μm. Subscripts such as 'c' and 'f' are referred to coarse and fine mode, respectively, and subscript 't' is referred to describe the total columnar volume size distribution including together the fine and coarse modes.

Increase of the coarse mode contribution to the daily average of columnar volume size distribution retrieved from direct Sun and diffuse sky radiance (in solar almucantar) is clearly seen from Figure 4. Radiance measurements were carried out at the Kishinev site on October 31, 2001. Peaks of volume modal radii for fine and coarse modes of volume size distribution were ~0.19 μm and ~1.71 μm, respectively. Ratio of volume concentrations of coarse and fine modes $C_{V,c}/C_{V,f}$ was ~3.5. In general, desert dust aerosols are highly inhomogeneous and variable depending on their origin, e.g. desert dust from the western part of Africa is strongly dominated by large aerosol particles and the ratio $C_{V,c}/C_{V,f}$ can reach the value of ~50, representing the case of so-called pure desert dust [9]. Variation of this ratio is highly dependent on contribution of fine mode sizes. For Kishinev case the relatively lower value of ratio $C_{V,c}/C_{V,f}$ (in comparison with the pure desert dust case) is due to increase of the contribution by fine mode sizes of urban aerosol of local origin and mixing of pollutions accumulated along the path of transport from Europe. For the case of desert dust, volume median sizes of fine $R_{V,f}$ and coarse $R_{V,c}$ modes are ~0.12-0.15 μm and ~ 1.9-2.54 μm , respectively [9]. For Kishinev case these values were $R_{V,f}$=0.19 μm and $R_{V,c}$ =2.06 μm, respectively, for observation day of October 31, 2001. The coarse mode of retrieved volume size distribution is likely related with the desert dust particles intrusion in Europe and their further transportation with the air masses from Europe to Moldova. The predominance of particles with size R> 0.6 μm in desert dust aerosols [9] is the basic feature to differentiate the optical properties of dust from the urban and biomass burning aerosols, which are characterized by dominant fine mode. The microphysical properties of retrieved column-integrated volume size distributions from the measurements carried out at the Kishinev site were compared with the analogous features retrieved from the observations made at the Leipzig site, Germany. These combined observations were carried out with an advanced Raman lidar and Sun photometer for detailed characterization of the microphysical and optical properties of a continental-scale intense Saharan dust intrusion observed over Leipzig from the 13th to 15th of October 2001 [18]. On October 30, 2001 the analogous dust intrusion has again originated from the Saharan desert region.

Table. 1. Microphysical characteristics of aerosol particles retrieved from direct Sun and sky radiance (in the solar almucantar) measurements on October 26 and 31, and November 5, 2001.

Parameters	26/10/2001	31/10/2001	05/11/2001
Coarse mode (c):			
R_v, μm	3.91	2.06	4.30
R_{eff}, μm	3.01	1.70	3.28
$C_{V,c}$, μm^3/ μm^2	0.016	0.134	0.015
Fine mode (f):			
R_v, μm	0.15	0.19	0.15
R_{eff}, μm	0.14	0.17	0.14
$C_{V,f}$, μm^3/ μm^2	0.010	0.038	0.013
Total (t):			
R_v, μm	1.18	1.21	0.98
R_{eff}, μm	0.35	0.56	0.29
C_V, μm^3/ μm^2	0.027	0.171	0.028

In frames of spheroid particle model used in retrieving procedure [15], the effective radii R_{eff} of the total volume size distribution for Leipzig and Kishinev site were ~ 0.59 μm and ~ 0.56 μm, respectively (Table 1). Negligible disagreement between values of the effective radius can be partly attributed to the fact that the Saharan dust event over Leipzig site from the 13th to 15th of October was rather intensive. At the same time, the next Saharan dust episode occurred on October 30 in Europe, had the less pronounced features: dust plume was in part transported by air masses from Europe to Moldova (Kishinev site) and it can be suggested that dust particles of coarse mode were partially removed by gravitational settling and mixed with the anthropogenic pollutions both of local origin and during the long-distance transport.

The other two size distributions, retrieved from the Sun/sky radiance measurements on October 26 and November 5, revealed the same structure with fine and coarse modes. Peaks of volume modal radius for fine and coarse modes of columnar volume size distribution for each day of observation, on October 26 and November 5, were ~0.15 µm and ~5.06 µm, respectively. Volume concentrations of coarse $C_{V,c}$ and fine $C_{V,f}$ modes for these days were lower than the analogous parameters specific for day on October 31. In particular, $C_{V,c}$ retrieved from measurements made on October 31 was higher than $C_{V,c}$ retrieved on October 26 and November 5, by about a factors of 8.3 and ~9, respectively. Retrieved columnar volume size distributions for these two days (Figure 4) have the resemblance of urban/industrial aerosol distributions [9]. Time series of the retrieved daily average values of volume concentration C_V for fine and coarse modes of sizes are shown in Figure 5.

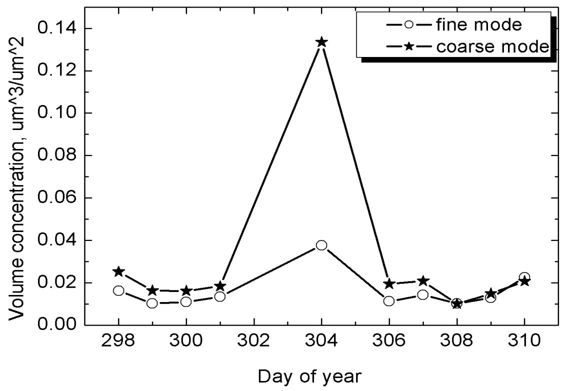

Figure 5. Time series of daily average values of volume concentration C_V for fine and coarse modes. Period of observation: from October 25, 2001 to November 6, 2001

Daily average values of AOT $<\tau_a(\lambda)>$ retrieved from the direct Sun radiance measurements at fixed wavelengths in the spectral range from 340 nm to 1020 nm are shown in Figure 6. Direct Sun radiance measurements were carried out on the 26th and 31st of October, and 5th of November. AOT $<\tau_a(\lambda)>$ retrieved from measurements on October 31 has a little spectral dependence and high absolute value that corresponds to the maximum influence of dust particles during the dust outbreak, when the air masses with dust particular matter were crossing over the Kishinev site.

Ångström exponent is a very good indicator of the size of the observed particles. Daily average values of the Angstrom exponent $<\alpha(440\_870)>$ were deduced from the direct Sun radiance measurements at λ= 440 , 500, 670, and 870 nm and by using linear regression analysis of the Ångström empirical expression $\tau_a(\lambda)=\beta\lambda^{-\alpha}$ [18]. Time series of daily average values of the Ångström exponent $<\alpha(440\_870)>$ is shown in Figure 7. From this Figure it is clearly seen the influence of desert dust particles with coarse mode sizes. The maximum influence of dust intrusion through the air masses transported to Moldova was observed on October 31, 2001. Daily average of AOT $<\tau_a(500)>$ amounted to ~ 0.36 and Ångström exponent $<\alpha(440\_870)>$ abruptly decreased to value of ~ 0.68. Monthly average values of the AOT $<\tau_a(500)>$ for October and November, 2001 consisted of values ~0.20 ± 0.13 and ~ 0.12 ± 0.08, respectively. At the same time, monthly average values of the Angstrom exponent $<\alpha(440\_870)>$ were ~1.36 ± 0.29 and ~1.40 ± 0.12, respectively, for these months. For the days prior to and after the dust event, Ångström exponent varied from 1.20 to 1.45, and AOT ranged from 0.07 to 0.10 . Column-integrated aerosol optical properties retrieved for these days had the resemblance with the urban/industrial type of aerosol [9].

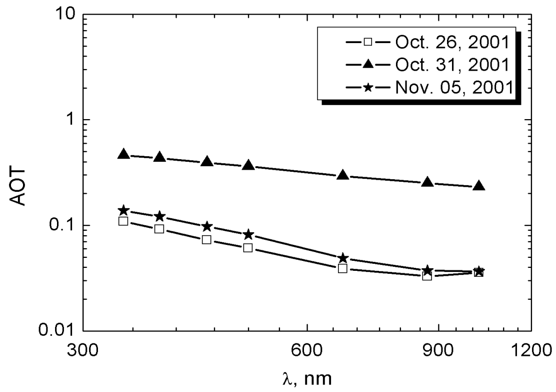

Figure 6. Spectral variation of daily average AOT $<\tau_a(\lambda)>$ for selected days of observation: on October 26, 31 and November 05, 2001 .

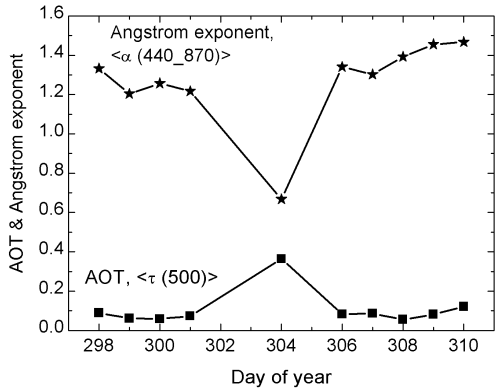

Figure 7. Time series of daily average values of AOT $<\tau_a(500)>$ at λ=500 nm and Angstrom exponent $<\alpha(440\_870)>$. Period of observation: from October 25, 2001 to November 6, 2001.

Spectral variability of retrieved daily average values of the single scattering albedo $<\omega_\lambda>$ for selected days of observation on October 26 an 31, and November 5, 2001, is shown in Figure 8. For the October 31, daily average values of $<\omega_\lambda>$ had a little spectral dependence and ranged from 0.94 at 440 nm to 0.95 at 1020 nm. Relatively high values of $<\omega_\lambda>$ may be attributed to the weak absorption of dust particulate matter. This day was characterized as the day, when the air masses with dust particles with the predominant contribution of the dust coarse mode component, have transported over the site of observation (Figure 4). For the days of observations on October 26 and November 5, prior to and after the dust event, respectively, retrieved single scattering albedos had distinct spectral dependence. In particular, on the 26th of October (a week prior to dust event) $<\omega_\lambda>$ ranged from 0.78 at 440 nm to 0.58 at 1020 nm, and on the 5th of November (a week after the dust event) $<\omega_\lambda>$ varied from 0.88 at 440 nm to 0.77 at 1020 nm. For all the days in time series, except for October 31(the 304-th day of year), retrieved daily average values of the single scattering albedo $<\omega_\lambda>$ revealed appreciable spectral dependence (Figure 9), being lower at longer wavelengths, which is a characteristic of both biomass burning aerosols and aerosols with anthropogenic origin [9].

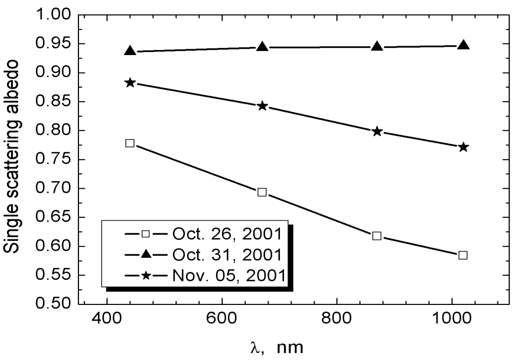

Figure 8.Spectral variability of daily average values of the single scattering albedo $<\omega_\lambda>$ for selected days of observation: on October 26, 31 and November 5, 2001 .

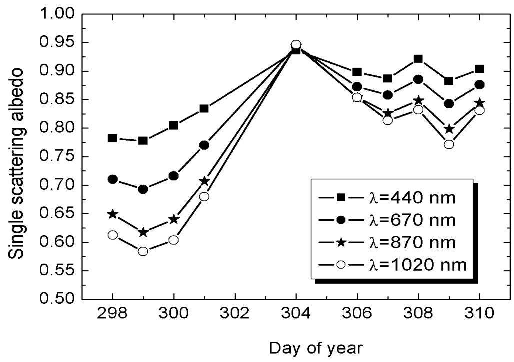

Figure 9. Time series of daily average values of the single scattering albedo $<\omega_\lambda>$. Period of observation: from October 25, 2001 to November 6, 2001.

Daily average values of the asymmetry factors for selected days of observation on October 26 and 31 , and November 5, 2001 revealed spectral dependence (Figure 10). Asymmetry factor retrieved on October 31 showed the larger values for all wavelengths in comparison with the retrieved one for other days. This fact indicates the presence and influence of a lot of particles with coarse mode sizes. The predominant radiation scattering in the forward hemisphere is typical for this case.

From time series of daily average of the imaginary part of complex refractive index of the particulate matter (Figure 11) it is seen the distinctive spectral dependence of *k(λ)* for all days except October 31, when *k(λ)* reached the minimum: variation of *k(λ)* at selected wavelengths from 440 nm to 1020 nm was negligible (see Table 2) , and *k(λ)* consisted of the value of ~ 0.0004 .

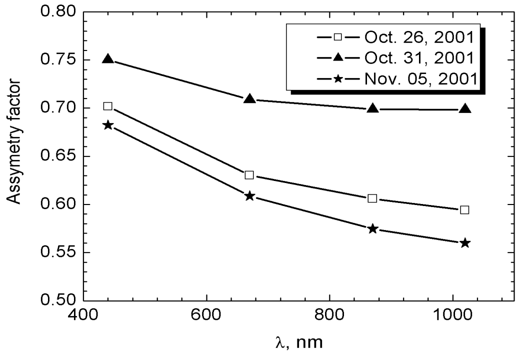

Figure 10. Spectral variability of daily average values of the asymmetry factors for selected days of observation: on October 26, 31 and November 05, 2001.

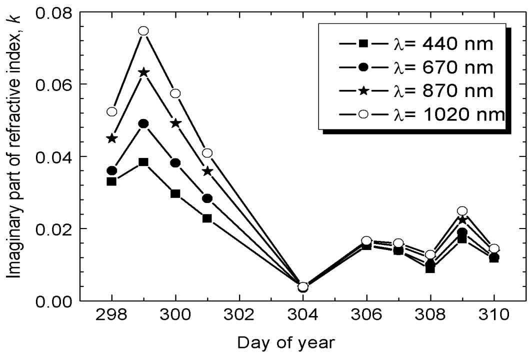

Figure 11. Time series of daily average values of the imaginary part of complex refractive index *m=n-ik*. Period of observation: from October 25, 2001 to November 6, 2001.

Daily average values of complex refractive indices *m=n-ik* of aerosol particles retrieved from direct Sun and diffuse sky radiance measurements for three selected days of observations are presented in Table 2. Some features concerning the retrieved values of the refractive index should be noted. Figure 11 shows the existence of spectral dependence for imaginary parts of refractive indices of particulate matter, *k(λ)*. This parameter, characterizing the absorption of medium, reduces from values ~0.038 – 0.075 before initiation and after termination of dust loading to values ~ 0.0035 – 0.0039 at the time of maximum influence of the dust pollution. Parameter *k(λ)* has the tendency to increase at longer wavelengths both before and after the dust event. This tendency of spectral dependence is inherent to the urban/industrial aerosols having the greater absorption than the dust [9]. Some negligible absorption can be attributed to mineral dust particles in the visible wavelength range.

Real part of refractive index, *n(λ)*, responsible for the scattering and this parameter, is also determined by aerosol composition. When the site was influenced by air masses with the dust transported from Europe, *n(λ)* acquired its smallest values ranging from 1.41 at 440 nm to 1.45 at 1020 nm. Before the dust event, *n(λ)* varied from 1.45 at 440 nm to 1.54 at 1020 nm and after this event *n(λ)* ranged from 1.49 at 440 nm to 1.54 at 1020 nm. High values of *n(λ)* can be prescribed to the contribution of urban/industrial aerosols to air masses transported from Europe [9]. Direct sampling and analysis of the complex refractive indices *m=n-ik* of individual aerosol particles in Europe region during the Lindenberg Aerosol Characterization experiment 1998 (LACE 98) showed variation of *n(λ)* from 1.51 to 1.58 , and *k(λ)* from 0.03 to 0.06 at 550 nm, depending on the amounts of soot and carbon/sulfate mixed particles [19].

Table. 2. Complex refractive index *m=n-ik* of aerosol particle matter retrieved from direct Sun and diffuse sky radiance almucantar measurements at wavelengths λ=440-, 670-, 870- and 1020 nm for three selected days of observations. Data retrieved are supplemented with daily mean temperature and relative humidity.

Parameters \ Date	26/10/2001	31/10/2001	05/11/2001
λ=440 nm	1.4517-i 0.0383	1.4093-i 0.0038	1.4858-i 0.0170
λ=670 nm	1.4683-i 0.0490	1.4351-i 0.0035	1.5034-i 0.0190
λ=870 nm	1.4955-i 0.0632	1.4462-i 0.0038	1.5173-i 0.0224
λ=1020 nm	1.5353-i 0.0747	1.4531-i 0.0039	1.5363-i 0.0249
Daily mean temperature, T ^{o}C	+2	+15	+7
Daily mean RH, %	64	68	64

Optical characteristics, such as complex refractive index *m=n-ik* and single scattering albedo ω_λ, retrieved from measurements at the wavelength λ=670 nm made at the Leipzig site, undergo variability: imaginary part of refractive index *k* is ~0.0014 – 0.004, real part of refractive index *n* is ~1.4 – 1.6, and single scattering albedo ω_λ is ~0.93 – 0.96 [18]. The analogous optical characteristics retrieved for Kishinev case are presented in Table 2. Single scattering albedo ω_λ for the Kishinev case is ~ 0.94 . It is clearly seen that these data show good agreement with the retrieved ones from measurements made at the Leipzig site.

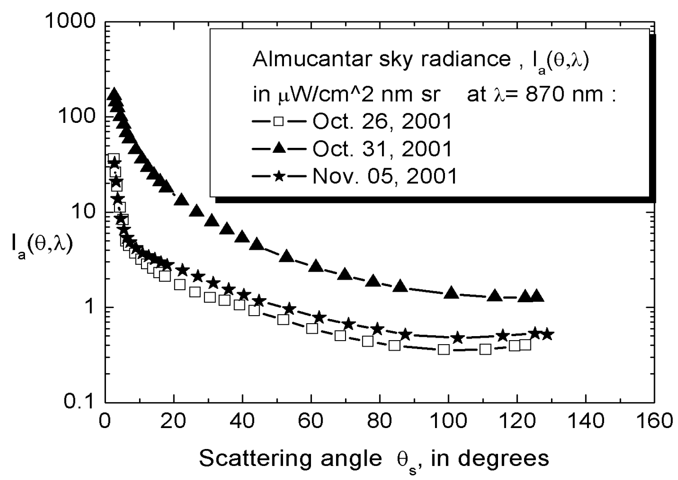

Figure 12. Time series variation of the diffuse sky radiance measured in the solar almucantar plane at λ=870 nm for set of scattering angles θ_s in the range from 3^o to 130^o.

Variation of measured diffuse sky radiances in the solar almucantar was examined for selected days: on October 26 and 31, and on November 5, 2001. The contribution of the dust particles with large sizes and concentrations results in increase and broadening of the forward lobe of scattering diagram for the set of scattering angles θ_S (relative to the Sun direction) ranged from 3^o to 20^o. In addition, it is clearly seen that the contribution of dust particles with coarse mode sizes leads to the modification of the whole diffuse sky radiance diagram $I_a(\theta,\lambda)$ for scattering angles θ_S in the range from 3^o to 130^o . Time series variation of the diffuse sky radiance measured in the solar almucantar is shown in Figure 12.

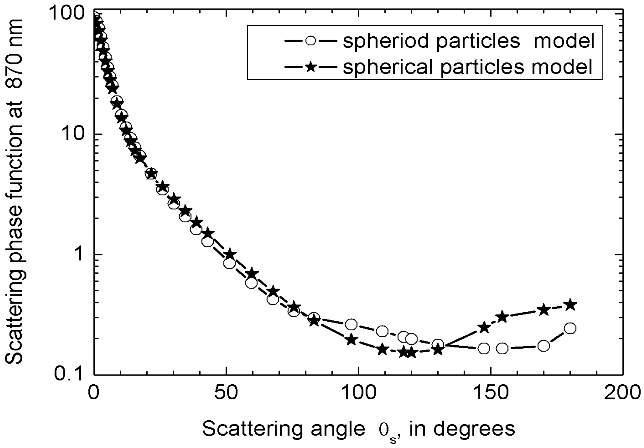

Figure 13. Variation of the scattering phase function computed at wavelength λ=870 nm for a set of scattering angles θ_S in the range from 0^o to 150^o .

Scattering phase functions at 870 nm derived from daily measurements on October 31, 2001 are shown in Fig 13. These functions were calculated on the basis of spherical (Mie scattering theory) and spheroidal particle models [15], respectively. The greatest discrepancy between the models is observed for scattering angles $\theta_S > 60^o$ (sideward and backward scattering). Use of the spheroidal particle model leads to increase of scattering phase function in the range of angles from 80^o to 130^o and to a significant decrease of phase function for scattering angles θ_S larger than 130^o .

4. Summary and conclusions

The present paper shows that the dust outbreak causes the essential variation of the columnar atmospheric aerosol optical and microphysical parameters. This influence is attributed to the amount of dust matter transported by air masses from Europe, where the dust has intruded from the Saharan desert regions. The results of direct Sun and diffuse sky radiance almucantar measurements, carried out during the dust outbreak from the Saharan and further long-range dust transport from Europe to Moldova for the period of observation from October 29 to November 5, 2001, illustrate the temporal variation of retrieved column-integrated aerosol optical thickness $\tau_a(\lambda)$, single scattering albedo $\omega_{\lambda,}$ Ångström exponent α(440_870), complex refractive index *m=n-ik*, and volume size distribution. At the Kishinev site the maximum influence of dust particles during the Saharan dust outbreak into Europe was registered on October 31, when the air masses with dust particulate matter were crossing Moldova.

Dust particle samples possessed a typical bimodal structure of the columnar volume size distributions with volume median radii R_V ~2.06 μm and ~0.19 μm, for coarse and fine modes, respectively. Corresponding volume concentrations C_V for these modes were ~ 0.134 and 0.038 $\mu m^3/\mu m^2$. Daily average value of AOT $<\tau_a(\lambda)>$ retrieved from measurements on October 31 had a little spectral dependence and high absolute value in comparison with other days. In particular, $<\tau_a(500)>$ amounted to ~ 0.36 on October 31. Monthly average values of the AOT $<\tau_a(500)>$ for October and November, 2001 were ~ 0.20 and ~0.12, respectively. During the day of dust event Ångström exponent $<\alpha(440\_870)>$ abruptly decreased to value of ~ 0.68, but for the days prior to and after the dust event Ångström exponent varied from 1.20 to 1.45 . On 31 October, daily average value of single scattering albedo $<\omega_\lambda>$ had a slight spectral dependence and it was ~0.94 at 440 nm, indicating the presence of dust particles. For other days $<\omega_\lambda>$ revealed appreciable spectral dependence, being lower at longer wavelengths, which is a characteristic of urban/industrial aerosols. On October 31 asymmetry factor showed the larger values for all wavelengths in comparison with other days. This was typical for the presence and influence of particles with coarse mode sizes and caused predominant radiation scattering in the forward hemisphere. At the day of dust event imaginary part of refractive index, *k(λ),* was ~ 0.0035–0.0039 with a little spectral dependence and real part of refractive index, *n(λ),* acquired the smallest values, which were ~1.41 at 440 nm and ~1.45 at 1020 nm.

Acknowledgements

I thank Dr. Brent Holben, the Principal Investigator of the AERONET program (NASA/GSFC) and his staff for the establishing sunphotometer Cimel-318 used in this investigation at the Kishinev site and data processing.

References

[1] Kaufman Y.J., D. Tanre, and O. Boucher, *Nature,* v. 419, 215-223 (2002).
[2] Intergovernmental Panel on Climate Change(IPCC), Climate Change 2001: the Scientific Basis, ed. by J.T. Houghton et al., Cambridge Univ. Press, New York (2001).
[3] Tegen I., A.A. Lacis, and I. Fung, *Nature,* v. 380, 419-422 (1996).
[4] Husar R.B., J.M. Prospero, L.L. Stowe, *J. Geophys. Res*., v.102, 16889-16909 (1997).
[5] Muller D., I. Mattis, U.Wandinger, A. Ansmann, D. Althausen, O. Dubovik, S. Eckhardt, and A. Stohl, *J. Geophys. Res*., v.108, 4345, doi:10.1029/2002JD002918 (2003).
[6] Holben B.N., et. al., *Rem. Sens. Environ.,* v.66, 1-16 (1998).
[7] Eck, T.F., B.N. Holben, J.S. Reid, O. Dubovik, A. Smirnov, N.T. O'Neill, I. Slutsker, and S. Kinne, *J. Geophys. Res*., v.104, 31333-31350 (1999).
[8] Smirnov A., B.N. Holben , I. Slutsker, E.J. Welton, and P. Formenti, *J. Geophys. Res.,* v.103, 28079-28092 (1998).
[9] Dubovik, O., B.N. Holben, T.F. Eck, A. Smirnov, Y.J. Kaufman, M.D. King, D. Tanre, and I. Slutsker, *J. Atmosph. Sci.,* v.59, 590-608 (2002).
[10] Coen M. , E. Weingartner , D. Schaub , C. Hueglin , C. Corrigan , M. Schwikowski , and U. Baltensperger, *Atmos. Chem. Phys. Discuss.,* 3, 5547–5594 (2003).
[11] Kubilay N., T. Cokacar, and T. Oguz, *J. Geophys. Res.,* v.108, 4666, doi:10.1029/2003JD003798 (2003).
[12] Smirnov A., B.N. Holben, T.F. Eck, O. Dubovik, and I. Slutsker, *Rem. Sens .Env*., v.73, 337-349 (2000).
[13] Dubovik, O. and M. D. King, *J. Geophys. Res*., v.105, 20673-20696 (2000).
[14] Dubovik, O., A.Smirnov, B.N. Holben, M.D. King, Y.J. Kaufman, T.F. Eck, and I. Slutsker, *J. Geophys. Res*., v.105, 9791-9806 (2000).
[15] Dubovik O., B.N. Holben, T. Lapyonok, A. Syniuk, M.I. Mishchenko, P. Yang, and I. Slutsker, *Geophys. Res. Lett.,* **29**, 54-1 - 54-4 (2002).
[16] Heintzenberg J., *Beitr. Phys. Atmos.,* v. 51, 91-99 (1998).
[17] Muller D., I. Mattis, U.Wandinger, A. Ansmann, D. Althausen, O. Dubovik, S. Eckhardt, and A. Stohl, *J. Geophys. Res*., v.108, 4345, doi:10.1029/2002JD002918 (2003).
[18] Angstrom, A., *Geogr. Ann.,* v.12, 130-159 (1929).
[19] Ebert, M., S. Weinbruch, A. Rausch, G. Gorzawski, G. Helas, P. Hoffmann, and H. Wex, *J. Geophys. Res*., v.107(D21), 8121, doi:10.1029/2000JD000195, (2002).